20

Laser diffractometry and measurement of the width of red blood cell size distribution

© S.Yu. Nikitin[1], E.G. Tsybrov[2], M.S. Lebedeva[1]

[1] Faculty of Physics, Moscow State University, Moscow, Russia
[2] Moscow State University, Faculty of Computational Mathematics and Cybernetics, Moscow, Russia

e-mail: tsybrovevgeniy@yandex.ru

Received July 31, 2024
Revised April 22, 2025
Accepted April 29, 2025

A new algorithm for measuring the width of erythrocyte size distribution based on the analysis of the diffraction pattern occurring in the far zone during the scattering of the laser beam on a blood smear is proposed. The algorithm is applicable to the analysis of weakly heterogeneous blood samples with symmetric size distribution function. The input data for the algorithm are the characteristics of the angular distribution of light intensity near the first dark ring in the diffraction pattern. The peculiarity of the algorithm is the reduced sensitivity to diffraction pattern noise, which is important for its experimental realization.

Keywords: laser diffractometry, blood smear, measurement of the width of red blood cell size distribution.

DOI: 10.61011/EOS.2025.07.61911.6944-25

Introduction

An important characteristic of blood is the relative width of the erythrocyte size distribution. Normally, this parameter, denoted as RDW (Red Blood Cell Distribution Width), is 12−14%, and its increase above this level indicates circulatory system disorders. Studies [1–3] emphasize the significance of the RDW parameter for assessing the general condition of the body and the likelihood of complications in various diseases.

The RDW parameter is part of a standard blood test. It is usually measured using automatic hematology analyzers equipped with a Coulter counter or by flow cytometry. However, these methods require complex equipment. An alternative method is laser diffractometry based on observing the scattering pattern of a laser beam on a blood smear. This method does not require complicated instrumentation and allows for fast measurements on large cell ensembles. Experimental studies on laser diffractometry of blood smears are presented in works [4–9]. Theoretical aspects of laser beam scattering by erythrocytes and their modeling particles are discussed in works [10–17]. Methods for measuring characteristics of erythrocyte size distribution based on laser diffractometry of blood smears are proposed in [7,18–21]. Practical implementation of such measurements requires high-quality diffraction patterns and video registration systems, as well as reliable and accurate data processing algorithms.

In this work, a new algorithm for measuring the width of erythrocyte size distribution is proposed, applicable to the analysis of weakly heterogeneous blood samples with symmetric size distribution functions. The input data for the algorithm are characteristics of the angular distribution of light intensity near the first dark ring in the diffraction pattern.

Experimental Data

In the experiments, we use wet blood smears. The erythrocytes are arranged in a thin liquid layer between the microscope slide and cover slip so that they form a sparse monolayer. An image of erythrocytes from a healthy donor obtained by microscope is shown in Fig. 1, *a*. Fig. 1, *b* shows the erythrocyte size (diameter) distribution measured by microscope for the sample of young healthy donor blood. As a measure of erythrocyte size spread, we take the quantity μ' defined by the formula

$$\mu' = \sqrt{\langle (D - \langle D \rangle)^2 \rangle} / \langle D \rangle.$$

Here, D is the diameter of an erythrocyte in the smear, and angular brackets denote averaging over the erythrocyte ensemble. The value μ' is dimensionless and convenient to express as a percentage. For example, for this blood sample $\mu' = 4.8\%$. Fig. 2, *a* shows the scheme of the experimental setup that includes a laser (*1*), the sample under study (*2*), a semi-transparent screen (*3*), and a digital camera (*4*).

Fig. 2, *b* shows the laser beam scattering pattern on the wet blood smear. Fig. 3 shows angular distribution of light intensity in this pattern. For analysis, we use the part of the diffraction pattern near the first dark ring. In experiments, we measure the angular coordinate of the first intensity minimum θ_0, the relative light intensity at the minimum f_0, and the relative curvature of the angular light intensity distribution f_2 at the coordinate θ_0. The meaning of these parameters is explained in Fig. 3. Mathematically, these

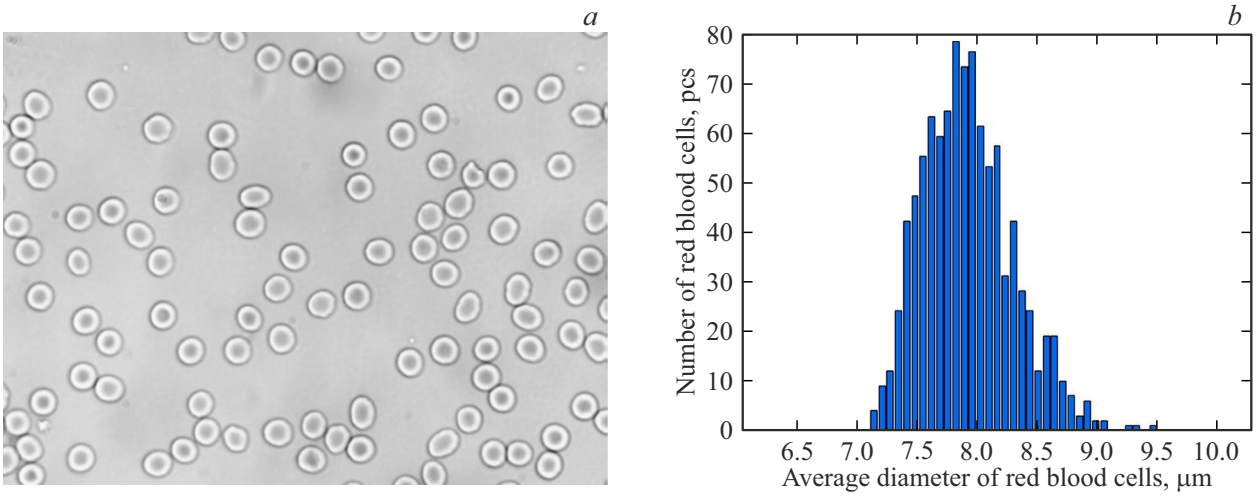

Figure 1. Microscopic view of blood smear (a) and erythrocyte size distribution (b).

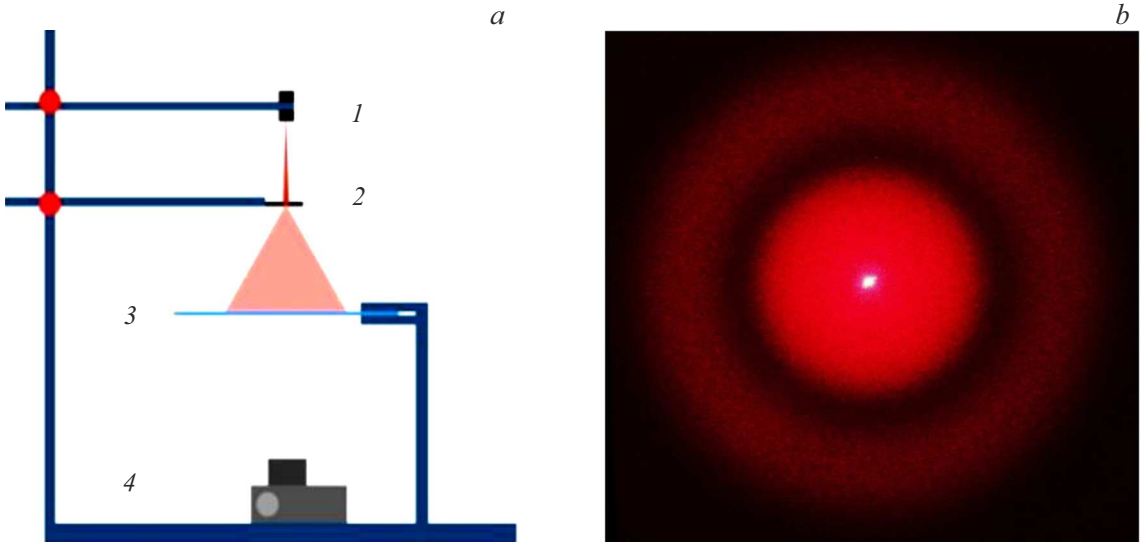

Figure 2. Experimental setup scheme for laser diffractometry of blood smear (a) and diffraction pattern view (b).

parameters are defined by formulas

$$f(\theta) = \frac{I(\theta)}{I(0)}, \quad f'(\theta_0) = 0,$$

$$f_0 = f(\theta_0), \quad f_2 = f''(\theta_0)\theta_0^2. \tag{1}$$

where I is the light intensity at the observation screen point and θ is the scattering angle.

Model of the Erythrocyte Ensemble

We consider the erythrocyte radius as a random variable described by the formula

$$R = R_0(1 + \varepsilon). \tag{2}$$

where R_0 is the mean erythrocyte radius, and ε is a random parameter with zero mean:

$$\langle \varepsilon \rangle = 0. \tag{3}$$

The width of the erythrocyte size distribution is characterized by the parameters

$$\mu = \langle \varepsilon^2 \rangle \tag{4}$$

and

$$\mu' = \sqrt{\mu}. \tag{5}$$

The parameter μ' characterizes the relative width of the erythrocyte size distribution. For a weakly heterogeneous ensemble, the parameter μ satisfies the condition.

$$\mu \ll 1. \tag{6}$$

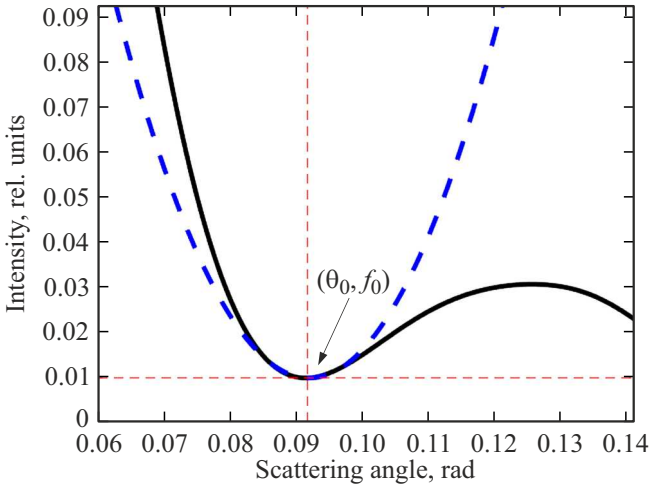

Figure 3. Angular distribution of light intensity in the diffraction pattern. Dashed lines show the parabolic approximation near the first minimum of intensity.

For blood samples close to those of healthy donors, condition (6) holds well. Our further task is to establish the relationship between parameters R_0 and μ' with measurable characteristics of the diffraction pattern θ_0, f_0, f_2. Based on this, we will develop algorithms to measure the mean erythrocyte radius and the width of the erythrocyte size distribution.

Angular Distribution of Light Intensity in the Diffraction Pattern

Using the results of work [21], the normalized angular distribution of light intensity in the diffraction pattern $f(\theta)$ is represented as

$$\frac{1}{4}\theta^2\langle\rho^4\rangle f(\theta) = \langle\rho^2 J_1^2(\rho\theta)\rangle. \tag{7}$$

where $I(0)$ is the intensity of the central maximum of the diffraction pattern, $\rho = kR$ is the wave parameter of erythrocyte size, R is the erythrocyte radius, $k = 2\pi/\lambda$ is the wave number, λ is the laser wavelength, and $J_1(x)$ is the first-order Bessel function. Angular brackets in formula (7) denote averaging over the erythrocyte ensemble. The intensity of the central maximum of the diffraction pattern is given by

$$I(0) = \frac{1}{4} I_0 N |\alpha|^2 \left(\frac{kR^2}{z}\right)^2.$$

Here, I_0 is incident laser beam intensity, N — number of erythrocytes irradiated by laser beam, z — distance from blood smear to observation screen $|\alpha|^2$ parameter characterizing erythrocyte thickness and optical density.

Model (7) is based on approximating an erythrocyte as a flat circular disk. Numerical calculations [17] for a biconcave disk show that the flat disk model provides good accuracy near the first dark ring of the diffraction pattern, which is the region used for analysis. Qualitatively, the pattern of laser beam scattering on a blood smear resembles the pattern of diffraction of a plane wave on a round hole (the so-called „Airy pattern“).

Homogeneous Ensemble Approximation

First, consider the special case of a homogeneous erythrocyte ensemble where $\rho = \rho_0 = \text{const}$. The expression for $f(\theta)$ simplifies to

$$\frac{1}{4}\rho_0^2 f(\theta) = \frac{1}{\theta^2} J_1^2(\rho_0\theta).$$

We calculate derivatives of the angular light intensity distribution with respect to the scattering angle

$$\frac{1}{8}\rho_0^2 f'(\theta) = -\frac{1}{\theta^3} J_1^2 + \frac{1}{\theta^2} J_1 J_1' \rho_0,$$

$$\frac{1}{8}\rho_0^2 f''(\theta) = \frac{3}{\theta^4} J_1^2 - \frac{4}{\theta^3} J_1 J_1' \rho_0 + \frac{\rho_0^2}{\theta^2}(J_1' J_1' + J_1 J_1'').$$

where the Bessel function argument is $\rho_0\theta$ and prime denotes derivative with respect to the entire argument. Let θ_0 be the angle where the first minimum of light intensity appears in the diffraction pattern. Then $f'(\theta_0) = 0$, from which $J_1(\rho_0\theta_0) = 0$and $\rho_0\theta_0 = x_0$are derived, where x_0 is the root of equation

$$J_1(x_0) = 0. \tag{8}$$

Denote

$$J_0(x_0) = -\beta. \tag{9}$$

It is known [22] that

$$x_0 = 3.8318, \quad \beta = 0.40276. \tag{10}$$

Assuming $\theta = \theta_0$, we get

$$f(\theta_0) = 0$$

and

$$f''(\theta_0)\theta_0^2 = 8 J_1'(x_0) J_1'(x_0).$$

Using expressions for Bessel function derivatives [22]

$$J_0'(x) = -J_1(x), \quad J_1'(x) = J_0(x) - \frac{1}{x} J_1(x), \tag{11}$$

we find

$$f''(\theta_0)\theta_0^2 = 8\beta^2.$$

denote for brevity

$$f(\theta_0) = f_0, \quad f'(\theta_0) = f_0', \quad f''(\theta_0)\theta_0^2 = f_2.$$

For the homogeneous erythrocyte ensemble case, we obtain

$$\rho = \rho_0, \ \theta_0 = \frac{x_0}{\rho_0}, \ f_0 = 0, \ f_0' = 0, \ f_2 = 8\beta^2. \tag{12}$$

where parameters x_0 and β are defined by formula (11). The erythrocyte radius in the blood smear can be found from formula

$$R_0 = x_0\lambda/2\pi\theta_0$$

or

$$R_0 = 0.61\,\frac{\lambda}{\theta_0}. \tag{13}$$

where λ is the laser wavelength and θ_0 is the scattering angle corresponding to the first minimum of light intensity on the diffraction pattern.

Diffractometric Equations

We now proceed to analyze the laser beam scattering by a size-heterogeneous erythrocyte ensemble. The equations relating the parameters of the diffraction pattern to the characteristics of the erythrocyte size distribution have the form

$$\frac{1}{4\beta^2}\,(1+\alpha)^2(1+6\mu)f_0 = \mu, \tag{14}$$

$$\frac{1}{\beta^2}\,(1+\alpha)(1+6\mu)f_0 = 2\alpha + 5\mu, \tag{15}$$

$$\frac{1}{\beta^2}\,(1+6\mu)\Big(f_0 + \frac{1}{8}\,f_2\Big) = 1 + 2(3-x_0^2)\mu. \tag{16}$$

Here, the diffraction pattern parameters f_0 and f_2 are defined by formulas (1), the numbers x_0 and β are defined by formulas (10), and the parameter μ is defined by formula (4). The parameter α is defined by the formula

$$\frac{\theta_0}{x_0}\rho_0 = 1 + \alpha, \tag{17}$$

where $\rho_0 = kR_0$ is the average erythrocyte size parameter. The parameter α describes the influence of the heterogeneity of the erythrocyte ensemble on the angular coordinate θ_0 of the first minimum of light intensity in the diffraction pattern. The derivation of equations (14)–(16) is given in the Appendix to this article.

Measurement Algorithms

From equations (14) and (15), it follows that

$$\alpha = -\frac{1}{2}\,\mu. \tag{18}$$

This approximate formula is valid under the assumption of a weakly heterogeneous erythrocyte ensemble when $\alpha, \mu \ll 1$. Substituting expression (18) into equations (15) and (16) gives We obtain

$$\Big(1 + \frac{11}{2}\,\mu\Big)f_0 = 4\beta^2\mu,$$

$$\frac{1}{\beta^2}(1+6\mu)\Big(f_0 + \frac{1}{8}\,f_2\Big) = 1 + 2(3-x_0^2)\mu.$$

From this, two algorithms for measuring parameter μ are obtained.

First algorithm:

$$\mu_1 = \frac{2f_0}{8\beta^2 - 11f_0},\ \ \mu_1' = \sqrt{\mu_1} = \sqrt{\frac{2f_0}{8\beta^2 - 11f_0}}.$$

Second algorithm:

$$\mu_2 = \frac{8\beta^2 - f_2}{2[8\beta^2(x_0^2-1) + 3f_2]},$$

$$\mu_2' = \sqrt{\mu_2} = \sqrt{\frac{8\beta^2 - f_2}{2[8\beta^2(x_0^2-1) + 3f_2]}}.$$

Or, taking into account (10):

$$\mu_1' = \sqrt{\frac{f_0}{0.649 - 5.5f_0}}, \tag{19}$$

$$\mu_2' = \sqrt{\frac{1.2977 - f_2}{35.52 + 6f_2}}. \tag{20}$$

Meanwhile, the average erythrocyte radius in the blood smear is determined by the formula

$$\rho_0 = (1 - 0.5\mu)\,\frac{3.83}{\theta_0}. \tag{21}$$

From it, the average erythrocyte diameter is

$$D_0 = \frac{\lambda}{\theta_0}\,\frac{3.83}{\pi}\Big(1 - \frac{1}{2}\,\mu\Big)$$

or

$$D_0 = 1.22\,\frac{\lambda}{\theta_0}\Big(1 - \frac{1}{2}\,\mu\Big).$$

Here, λ is the laser wavelength, θ_0 is the angular coordinate of the light intensity minimum in the diffraction pattern, and the parameter μ corresponds to the square of the erythrocyte size distribution width.

Verification of Algorithms by Numerical Experiment

The verification of the algorithm generally proceeds as follows. The parameters of the erythrocyte ensemble are set. The direct scattering problem is solved. Parameters of the diffraction pattern are found. These parameters are input into the algorithm for solving the inverse scattering problem. Parameters of the erythrocyte ensemble are obtained and compared with the initially set parameters. This allows assessment of the algorithm's functionality and accuracy, and determination of its applicability regarding permissible ensemble heterogeneity.

We used a model of a symmetric bimodal ensemble (BME), where the sample contains equal amounts of two cell types with size parameters ρ_1 and ρ_2 to verify the

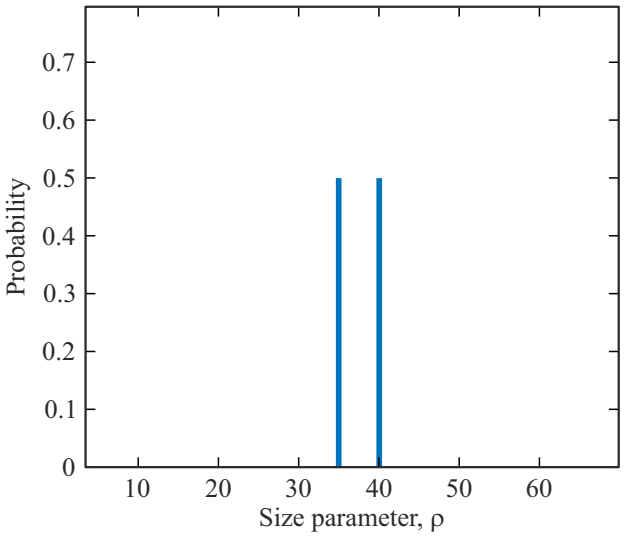

Figure 4. Bimodal erythrocyte ensemble erythrocyte size distribution.

algorithms. An example of the bimodal distribution is shown in Fig. 4. Exact parameter values of such an ensemble are defined by formulas

$$\rho_0 = \frac{1}{2}(\rho_1 + \rho_2), \quad \mu = \langle \varepsilon^2 \rangle = \frac{1}{2}(\varepsilon_1^2 + \varepsilon_2^2),$$

$$\rho_1 = \rho_0(1 + \varepsilon_1), \quad \rho_2 = \rho_0(1 + \varepsilon_2).$$

From these,

$$\mu = \left(\frac{\rho_2 - \rho_1}{\rho_1 + \rho_2}\right)^2, \ \mu' = \sqrt{\mu} = \frac{\rho_2 - \rho_1}{\rho_1 + \rho_2}.$$

For the symmetric BME, the normalized angular distribution of light intensity in the diffraction pattern is described by the formula

$$f(\theta) = \frac{4[\rho_1^2 J_1^2(\rho_1\theta) + \rho_2^2 J_1^2(\rho_2\theta)]}{(\rho_1^4 + \rho_2^4)\theta^2}.$$

We found the coordinate of the minimum of this function $\theta = \theta_0$ and determined the parameters $f_0 = f(\theta_0)$ and $f_2 = f''(\theta_0)\theta_0^2$. Five different bimodal ensembles differing in size distribution width (μ') were considered. The obtained data are presented in Table 1. In this table, ρ_1 is the size parameter of the first ensemble component, ρ_2 is the size parameter of the second component, p is the fraction of the first type particles, ρ_0 is the average size parameter of the particle ensemble, μ' is the particle size spread, θ_0 is the angular coordinate of the first minimum of light intensity in the diffraction pattern, f_0 is the relative intensity of the first minimum, and, f_2 is the normalized curvature of the angular intensity distribution near the first minimum in the diffraction pattern.

These data were used as input parameters for algorithms (19)–(21). The calculation results according to formulas (19)–(21) are shown in Table 2. Here, ρ_0 is the exact

Table 1. Parameters of diffraction patterns found by the numerical experiment method.

Parameters	BME1	BME2	BME3	BME4	BME5
ρ_1	35	34	33	32	31
ρ_2	40	41	42	43	44
p	0.5	0.5	0.5	0.5	0.5
ρ_0	37.5	37.5	37.5	37.5	37.5
μ', %	6.67	9.33	12.0	14.7	17.3
θ_0, rad	0.102	0.102	0.101	0.101	0.100
f_0	0.00275	0.00515	0.00802	0.0111	0.0143
f_2	1.12	0.955	0.760	0.556	0.354

Table 2. Calculation results

Calculated Parameters	BME1	BME2	BME3	BME4	BME5
ρ_0	37.5	37.5	37.5	37.5	37.5
ρ_{0a}	37.5	37.4	37.7	37.5	37.7
μ', %	6.67	9.33	12.0	14.7	17.3
μ_1', %	6.59	9.11	11.5	13.7	15.8
μ_2', %	6.49	9.11	11.6	13.8	15.8

average size parameter for the bimodal particle ensemble, ρ_{0a} is the average size parameter found from analysis of the diffraction pattern by algorithm (21), μ' is the exact particle size spread, μ_1' is the size spread found by analysis of the diffraction pattern using algorithm (19), μ_2' particle size distribution found by analyzing the diffraction pattern using an algorithm (20). Table 2 shows that with accurate input data, the algorithm errors do not exceed 10% in the region $\mu' \leq 17\%$.

Analysis of Diffraction Pattern Noise Influence

In practice, the diffraction pattern always contains a random (noise) component. Noise may arise from characteristics of the laser and diffraction pattern video registration system, scattering of the laser beam on dust particles, etc. Therefore, it is important to evaluate the robustness of the proposed data processing algorithms against noise in the diffraction pattern. We conducted this study by numerical experiment. The angular distribution of light intensity in the diffraction pattern was modeled by the function

$$f(\theta) = \frac{4[\rho_1^2 J_1^2(\rho_1\theta) + \rho_2^2 J_1^2(\rho_2\theta)]}{(\rho_1^4 + \rho_2^4)\theta^2} + \xi(\theta),$$

where $\xi(\theta)$ is a random function of the scattering angle with probability density distribution

$$w(\xi) = \begin{cases} \frac{1}{\xi_0}, \text{ if } 0 \leq \xi \leq \xi_0, \\ 0, \text{ if } \xi < 0, \xi > \xi_0. \end{cases}$$

Table 3. Analysis of the influence of diffraction pattern noise

Parameters of calculated diffraction patterns	BME1	BME2	BME3	BME4	BME5
θ_0, rad	0.102	0.101	0.101	0.101	0.101
f_0	0.00533	0.00767	0.0105	0.0136	0.0168
f_2	1.101	0.902	0.749	0.550	0.379
μ', %	6.67	9.33	12.0	14.7	17.3
μ'_1, %	9.3	11.2	13.3	15.4	17.3
μ'_2, %	6.8	9.8	11.7	13.9	15.6

Here, values of this function at different scattering angles were considered statistically independent (spatial white noise). In practice, in the region of interest in the diffraction pattern, noise intensity weakly depends on the scattering angle. Thus, the spatial white noise model is adequate for the experimental conditions. For numerical calculations, the parameters ρ_1 and ρ_2 were taken equal to values shown in Table 1. Calculations were conducted for noise parameter values ξ_0 equal to 0.001, 0.002, 0.003, 0.004, 0.005. Table 3 presents the parameters θ_0, f_0, f_2 of the calculated diffraction patterns for noise level $\xi_0 = 0.005$ and corresponding calculation results of parameters μ'_1 and μ'_2 using formulas (19) and (20).

Discussion of Results

This paper presents a new algorithm for measuring the width of the erythrocyte size distribution using laser diffractometry of blood smears. The main result is expressed in formulas (19) and (20). In these formulas, μ' is the width of the erythrocyte size distribution, f_0 and f_2 are parameters of the diffraction pattern formed by laser beam scattering on the blood smear. Both parameters characterize the angular light intensity distribution near the first minimum of intensity in the diffraction pattern. This region corresponds to the dark ring surrounding the central maximum. Parameter f_0 is the relative light intensity at the first minimum, and f_2 represents the relative curvature of the angular intensity distribution near the first minimum in the diffraction pattern. Mathematically, μ', f_0 and f_2 are defined by formulas (1)–(5). Algorithms (19) and (20) apply to analysis of weakly heterogeneous blood samples with symmetric size distribution functions.

Using numerical experiments, we evaluated the accuracy of algorithms (19) and (20), with results shown in Table 2. The analysis demonstrated that with accurate input data, algorithm errors do not exceed 10% in the region $\mu' \leq 17\%$.

We also studied algorithm robustness against diffraction pattern noise, shown in Table 3. The data indicate that for ensembles with erythrocyte size spread $7\% \leq \mu' \leq 17\%$ and noise level $\xi_0 = 0.005$ algorithm (20) error does not exceed 9.8%, while algorithm (19) error reaches 39.4%. Thus, algorithm (20) shows weaker sensitivity to diffraction pattern noise than algorithm (19). Note also that algorithm (20), unlike (19), does not require photometry of the diffraction pattern over a wide angular range, simplifying the measurement procedure.

Appendix

Derivation of Diffractometric Equations

We use the equation for the normalized angular distribution of light intensity in the diffraction pattern $f(\theta)$:

$$\frac{1}{4}\langle\rho^4\rangle\theta^2 f = \langle\rho^2 J_1^2\rangle.$$

where $J_1 = J_1(\rho\theta)$ is the first-order Bessel function, ρ is the erythrocyte size parameter (random variable), and angular brackets denote averaging over the erythrocyte ensemble. Differentiating the right and left sides of this equality with respect to the scattering angle θ, we obtain the equations

$$\frac{1}{8}\langle\rho^4\rangle(2f + \theta f')\theta = \langle\rho^3 J_1 J_1'\rangle,$$

$$\frac{1}{8}\langle\rho^4\rangle(2f + 4\theta f' + \theta^2 f'') = \langle\rho^4 J_1 J_1''\rangle + \langle\rho^4 J_1' J_1'\rangle.$$

Using formulas (11), we eliminate the derivatives of the Bessel functions from the equations. We obtain

$$\frac{1}{4}\langle\rho^4\rangle f\theta^2 = \langle\rho^2 J_1 J_1\rangle,$$

$$\frac{1}{8}\langle\rho^4\rangle(2f + \theta f')\theta = \langle\rho^3 J_1 J_0\rangle - \frac{1}{\theta}\langle\rho^2 J_1 J_1\rangle,$$

$$\frac{1}{8}\langle\rho^4\rangle(2f + 4\theta f' + \theta^2 f'') = \frac{3}{\theta^2}\langle\rho^2 J_1 J_1\rangle - \langle\rho^4 J_1 J_1\rangle - \frac{3}{\theta}\langle\rho^3 J_1 J_0\rangle + \langle\rho^4 J_0 J_0\rangle.$$

Consider the region of the diffraction pattern close to the first minimum of light intensity. Using notation (1) and assuming $\theta = \theta_0$, we get

$$\frac{1}{4}\langle\rho^4\rangle f_0\theta_0^2 = \langle\rho^2 J_1 J_1\rangle,$$

$$\frac{1}{4}\langle\rho^4\rangle f_0\theta_0 = \langle\rho^3 J_1 J_0\rangle - \frac{1}{\theta_0}\langle\rho^2 J_1 J_1\rangle,$$

$$\frac{1}{8}\langle\rho^4\rangle(2f_0 + f_2) = \frac{3}{\theta_0^2}\langle\rho^2 J_1 J_1\rangle - \langle\rho^4 J_1 J_1\rangle - \frac{3}{\theta_0}\langle\rho^3 J_1 J_0\rangle + \langle\rho^4 J_0 J_0\rangle$$

or

$$\frac{1}{4}\langle\rho^4\rangle f_0\theta_0^2 = \langle\rho^2 J_1 J_1\rangle,$$

$$\frac{1}{2}\langle\rho^4\rangle f_0\theta_0 = \langle\rho^3 J_1 J_0\rangle,$$

$$\langle\rho^4\rangle f_0 + \frac{1}{8}\langle\rho^4\rangle f_2 = \langle\rho^4 J_0 J_0\rangle - \langle\rho^4 J_1 J_1\rangle. \quad \text{A1}$$

Here, the argument of the Bessel functions is the quantity $x = \rho\theta_0$.

We write approximate expressions for the Bessel functions near the point $x = x_0$, defined by condition (8). Expanding the functions in a Taylor series, we obtain

$$J_0(x) = -a_3 y^3 + a_2 y^2 - a_1 y + a_0,$$

$$J_1(x) = b_3 y^3 - b_2 y^2 + b_1 y - b_0.$$

Here, the expansion coefficients are defined by the formulas

$$a_3 = \frac{\beta}{6}x_0^2,\ a_2 = \frac{\beta}{6}6x_0^2,\ a_1 = \frac{\beta}{6}9x_0^2,\ a_0 = \frac{\beta}{6}2(2x_0^2 - 3), \quad \text{(A2)}$$

$$b_3 = \frac{\beta}{6}x_0(x_0^2 - 3),\ b_2 = \frac{\beta}{6}x_0 3(x_0^2 - 4),$$

$$b_1 = \frac{\beta}{6}x_0 3(x_0^2 - 7),\ b_0 = \frac{\beta}{6}x_0(x_0^2 - 12)$$

and

$$y = \frac{\rho\theta_0}{x_0}. \quad \text{(A3)}$$

In the same approximation, bilinear combinations of Bessel functions are given by the formulas

$$J_0 J_0 = c_{06}y^6 - c_{05}y^5 + c_{04}y^4 - c_{03}y^3 + c_{02}y^2 - c_{01}y + c_{00},$$

$$J_1 J_1 = c_{16}y^6 - c_{15}y^5 + c_{14}y^4 - c_{13}y^3 + c_{12}y^2 - c_{11}y + c_{10},$$

$$J_0 J_1 = -c_{26}y^6 + c_{25}y^5 - c_{24}y^4 + c_{23}y^3 - c_{22}y^2 + c_{21}y - c_{20}. \quad \text{(A4)}$$

Here,

$$c_{06} = a_3^2,\ c_{05} = 2a_3a_2,\ c_{04} = 2a_3a_1 + a_2^2,$$

$$c_{03} = 2(a_3a_0 + a_2a_1),$$

$$c_{02} = 2a_2a_0 + a_1^2,\ c_{01} = 2a_1a_0,\ c_{00} = a_0^2,$$

$$c_{16} = b_3^2,\ c_{15} = 2b_3b_2,\ c_{14} = 2b_3b_1 + b_2^2,$$

$$c_{13} = 2(b_3b_0 + b_2b_1),$$

$$c_{12} = 2b_2b_0 + b_1^2,\ c_{11} = 2b_1b_0,\ c_{10} = b_0^2,$$

$$c_{26} = a_3b_3,\ c_{25} = a_3b_2 + a_2b_3,$$

$$c_{24} = a_3b_1 + a_2b_2 + a_1b_3,$$

$$c_{23} = a_3b_0 + a_2b_1 + a_1b_2 + a_0b_3,$$

$$c_{22} = a_2b_0 + a_1b_1 + a_0b_2,$$

$$c_{21} = a_1b_0 + a_0b_1,\ c_{20} = a_0b_0. \quad \text{(A5)}$$

Using notation (A3), rewrite equations (A1) in the form

$$\frac{1}{4}\langle y^4\rangle f_0 x_0^2 = \langle y^2 J_1 J_1\rangle,$$

$$\frac{1}{2}\langle y^4\rangle f_0 x_0 = \langle y^3 J_1 J_0\rangle,$$

$$\langle y^4\rangle f_0 + \frac{1}{8}\langle y^4\rangle f_2 = \langle y^4 J_0 J_0\rangle - \langle y^4 J_1 J_1\rangle. \quad \text{(A6)}$$

Here, angular brackets denote averaging over the random variable y, proportional to the erythrocyte size parameter. Using formula (2), we get

$$y = \frac{\rho_0\theta_0}{x_0}(1 + \varepsilon),$$

where $\rho_0 = kR_0$ is the average erythrocyte size parameter. In the homogeneous ensemble approximation, the angle θ_0 depends only on the erythrocyte size ρ_0. If the ensemble is heterogeneous, then the angle θ_0 at which the minimum of light intensity is seen in the diffraction pattern, depends on the average erythrocyte size ρ_0 as well as on the width of the erythrocyte size distribution. For a weakly heterogeneous ensemble, we represent this dependence as

$$\frac{\rho_0\theta_0}{x_0} = 1 + \alpha,$$

where α is a small parameter to be determined. Now

$$y = (1 + \alpha)(1 + \varepsilon). \quad \text{(A7)}$$

Here, α and ε are small parameters, i.e.

$$|\alpha| \ll 1, \quad |\varepsilon| \ll 1. \quad \text{(A8)}$$

Note that only parameter ε is random. Its characteristic is the variance $\langle\varepsilon^2\rangle = \mu$. The other moments of parameter ε in our adopted model are assumed zero:

$$\langle\varepsilon^n\rangle = \begin{cases}\mu, n = 2,\\ 0, n = 1, 3, \ldots\end{cases}.$$

Substituting expression (A7) into equations (A6), we obtain

$$\frac{1}{4}(1 + \alpha)^2\langle(1 + \varepsilon)^4\rangle f_0 x_0^2 = \langle(1 + \varepsilon)^2 J_1 J_1\rangle,$$

$$\frac{1}{2}(1 + \alpha)\langle(1 + \varepsilon)^4\rangle f_0 x_0 = \langle(1 + \varepsilon)^3 J_1 J_0\rangle,$$

$$\langle(1 + \varepsilon)^4\rangle\left(f_0 + \frac{1}{8}f_2\right) = \langle(1 + \varepsilon)^4 J_0 J_0\rangle - \langle(1 + \varepsilon)^4 J_1 J_1\rangle. \quad \text{(A9)}$$

Neglecting powers of parameter ε higher than second order, we obtain

$$(1 + \varepsilon)^n = 1 + n\varepsilon + \frac{1}{2}n(n - 1)\varepsilon^2.$$

In particular,

$$(1 + \varepsilon)^2 = 1 + 2\varepsilon + \varepsilon^2,\ (1 + \varepsilon)^3 = 1 + 3\varepsilon + 3\varepsilon^2,$$

$$(1 + \varepsilon)^4 = 1 + 4\varepsilon + 6\varepsilon^2.$$

From these,

$$\langle(1 + \varepsilon)^4\rangle = 1 + 6\mu.$$

Equations (A9) take the form

$$\frac{1}{4}(1+\alpha)^2(1+6\mu)f_0x_0^2 = \langle(1+2\varepsilon+\varepsilon^2)J_1J_1\rangle,$$
$$\frac{1}{2}(1+\alpha)(1+6\mu)f_0x_0 = \langle(1+3\varepsilon+3\varepsilon^2)J_1J_0\rangle,$$
$$(1+6\mu)\Big(f_0+\frac{1}{8}f_2\Big) = \langle(1+4\varepsilon+6\varepsilon^2)J_0J_0\rangle - \langle(1+4\varepsilon+6\varepsilon^2)J_1J_1\rangle$$

or

$$\frac{1}{4}(1+\alpha)^2(1+6\mu)f_0x_0^2 = \langle J_1J_1\rangle + 2\langle\varepsilon J_1J_1\rangle + \langle\varepsilon^2J_1J_1\rangle,$$
$$\frac{1}{2}(1+\alpha)(1+6\mu)f_0x_0 = \langle J_1J_0\rangle + 3\langle\varepsilon J_1J_0\rangle + 3\langle\varepsilon^2J_1J_0\rangle,$$
$$(1+6\mu)\Big(f_0+\frac{1}{8}f_2\Big) = \langle J_0J_0\rangle + 4\langle\varepsilon J_0J_0\rangle + 6\langle\varepsilon^2J_0J_0\rangle - \langle J_1J_1\rangle - 4\langle\varepsilon J_1J_1\rangle - 6\langle\varepsilon^2J_1J_1\rangle. \quad \text{(A10)}$$

To calculate the averages, we use approximate expressions

$$\langle y^n\rangle = 1+n\alpha+\frac{1}{2}n(n-1)\mu,\ \langle\varepsilon y^n\rangle = n\mu,\ \langle\varepsilon^2y^n\rangle = \mu,$$

valid under conditions (A8).

Next, we use formulas for coefficients c_0, c_1, c_2 derived from (A2) and (A4):

Coefficients c_0 (for brevity, multipliers are omitted $(\beta/6)^2$):

$$c_{06} = x_0^4,\ c_{05} = 12x_0^4,\ c_{04} = 54x_0^4,\ c_{03} = 4x_0^2(29x_0^2-3),$$
$$c_{02} = 3x_0^2(43x_0^2-24),\ c_{01} = 36x_0^2(2x_0^2-3),$$
$$c_{00} = 4(4x_0^4-12x_0^2+9);$$

Coefficients c_1 (for brevity, multipliers are omitted $x_0^2(\beta/6)^2$):

$$c_{16} = x_0^4-6x_0^2+9,\ c_{15} = 6(x_0^4-7x_0^2+12),$$
$$c_{14} = 3(5x_0^4-44x_0^2+90),$$
$$c_{13} = 4(5x_0^4-57x_0^2+144),\ c_{12} = 3(5x_0^4-74x_0^2+243),$$
$$c_{11} = 6(x_0^4-19x_0^2+84),\ c_{10} = (x_0^4-24x_0^2+144);$$

Coefficients c_2 (for brevity, multipliers are omitted $(\beta/6)^2$):

$$c_{26} = x_0^3(x_0^2-3),\ c_{25} = 3x_0^3(3x_0^2-10),$$
$$c_{24} = 30x_0^3(x_0^2-4),\ c_{23} = 2x_0^3(25x_0^2-132)+18x_0,$$
$$c_{22} = 3x_0^3(15x_0^2-109)+72x_0,$$
$$c_{21} = 21x_0^3(x_0^2-10)+126x_0,$$
$$c_{20} = 2x_0^3(2x_0^2-27)+72x_0.$$

Using these formulas, we find

$$\langle J_1J_1\rangle = x_0^2\beta^2\mu,\ \langle\varepsilon J_1J_1\rangle = 0,\ \langle\varepsilon^2J_1J_1\rangle = 0,$$
$$\langle J_1J_0\rangle = \Big(\alpha x_0-\frac{1}{2}x_0\mu\Big)\beta^2,$$
$$\langle\varepsilon J_1J_0\rangle = \beta^2x_0\mu,\ \langle\varepsilon^2J_1J_0\rangle = 0,\ \langle J_0J_0\rangle = (1-x_0^2\mu)\beta^2,$$
$$\langle\varepsilon J_0J_0\rangle = 0,\ \langle\varepsilon^2J_0J_0\rangle = \beta^2\mu. \quad \text{(A11)}$$

Substituting expressions (A11) into equations (A10), we obtain equations (14)–(16).

Funding

The theoretical part, development of the numerical experiment methodology, and data analysis were supported by the Russian Science Foundation grant (№ 22-15-00120). Computer modeling of diffraction patterns was supported by the Ministry of Education and Science of the Russian Federation under the Moscow Center for Fundamental and Applied Mathematics program by agreements № 075-15-2022-284 and № 075-15-2025-345.

Conflict of interest

The authors declare that they have no conflict of interest.

References

[1] K.V. Patel, R.D. Semba, L. Ferrucci, A.B. Newman, L.P. Fried, R.B. Wallace et al. Biological Sciences and Medical Sciences, *65A* (3), 258–265 (2010). DOI: 10.1093/gerona/glp163

[2] S. Huang, Q. Zhou, N. Guo, Z. Zhang, L. Luo, Y. Luo et al. Medicine (Baltimore), **100** (15), e25404 (2021). DOI: 10.1097/MD.0000000000025404

[3] N.A. Karanadze, Yu.L. Begrambekova, E.N. Borisov, Ya.A. Orlova. Kardiologiya, **62** (4), 30–35 (2022). DOI: 10.18087/cardio.2022.4.n1813 (in Russian)

[4] Ye Yang, Zhenxi Zhang, Xinhui Yang, Joon Hock Yeo, Li Jun Jiang, Dazong Jiang. J. Biomed. Optics, **9** (5), 995–1001 (2004). DOI: 10.1117/1.1782572

[5] E.T. Aksenov, D.V. Mokrova. Pis'ma v ZhTF, **34** (20), 38 (2008) (in Russian).

[6] M. Kinnunen, A. Kauppila, A. Karmenyan, R. Myllylä. Biomed. Opt. Express, **2** (7), 1803–1814 (2011). DOI: 10.1364/BOE.2.001803

[7] Yu.S. Yurchuk, V.D. Ustinov, S.Yu. Nikitin, A.V. Priezzhev. Kvant. elektron., **46** (6), 515–520 (2016) (in Russian). DOI: 10.1070/QEL16108

[8] A.E. Shtan'ko, G.S. Kalenkov, A.E. Lugovtsov, M.A. Karpilova. Meditsinskaya tekhnika, **1** 5–6 (2020) (in Russian).

[9] M.S. Lebedeva, E.G. Tsybrov, A.E. Nikandrova. V sb.: it Trudy XVI Mezhdunarodnoj nauchno-tekhnicheskoj konferencii glqq Opticheskie metody issledovaniya potokov (Pero, M., 2021), p. 175–182. (in Russian)

[10] C.E.T. Krakau. Biophys. J., **6**, 801–811 (1966). DOI: 10.1016/S0006-3495(66)86696-1

[11] G.J. Streekstra, A.G. Hoekstra, E.-J. Nijhof, R.M. Heethaar. Appl. Opt., **32** (13), 2266–2272 (1993). DOI: 10.1364/AO.32.002266

[12] A.G. Borovoi, E.I. Naats, U.G. Oppel. J. Biomed. Opt., **3** (3), 364–72 (1998). DOI: 10.1117/1.429883

[13] E. Eremina, Y. Eremin, W. Thomas. Opt. Commun., **244**, 15–23 (2005). DOI: 10.1016/j.optcom.2004.09.037.

[14] P. Tarasov, M. Yurkin, P. Avrorov, K. Semyanov, A. Hoekstra, V. Maltsev. *Optics of Biological Particles*, ed. by A. Hoekstra et al. (Springer, 2007), p. 243–259. DOI: 10.1007/978-1-4020-5502-7_8

[15] A.V. Priezzhev, S.Yu. Nikitin, A.E. Lugovtsov. J. Quantitative Spectroscopy and Radiative Transfer, **110**, 1535 (2009). DOI: 10.1016/j.jqsrt.2009.02.027

[16] S.Yu. Nikitin, A.E. Lugovtsov, A.V. Priezzhev. Kvant. elektron. (in Russian), **40** (12), 1074–1076 (2010).
[17] S.Yu. Nikitin, A.V. Priezzhev, A.E. Lugovtsov. J. Quantitative Spectroscopy and Radiative Transfer, **121**, 1–8 (2013). DOI: 10.1016/j.jqsrt.2013.02.014
[18] S.Yu. Nikitin, A.E. Lugovtsov, A.V. Priezzhev, V.D. Ustinov. Kvant. elektron., **41** (9), 843–846 (2011) (in Russian).
[19] V.D. Ustinov, E.G. Tsybrov. Inverse Problems in Science and Engineering, **28** (11), 1633–1647 (2020). DOI: 10.1080/17415977.2020.1761801
[20] S.Yu. Nikitin, V.D. Ustinov, E.G. Tsybrov, M.S. Lebedeva. Opt. i spektr., **129** (7), 961–971 (2021) (in Russian). DOI: 10.21883/OS.2021.07.51089.269-20
[21] S.Yu. Nikitin, E.G. Tsybrov, M.S. Lebedeva, A.E. Lugovtsov, A.V. Priezzhev. Kvant. elektron., **52** (7), 664–670 (2022) (in Russian).
[22] E. Yanke, F. Emde, F. Lyosh.
it Special'nye funkcii (Nauka, M., 1977). (in Russian)

Translated by J.Savelyeva